Available online at www.sciencedirect.com
SCIENCE DIRECT®
Fluid Dynamics Research 38 (2006) 241–256
FLUID DYNAMICS RESEARCH

A stable moving-particle semi-implicit method for free surface flows

B. Ataie-Ashtiani*, Leila Farhadi

Department of Civil Engineering, Sharif University of Technology, P.O. Box 11365-9313, Tehran, Iran

Received 11 August 2004; received in revised form 30 August 2005; accepted 6 December 2005

Communicated by M. Oberlack

Abstract

In this paper, a mesh-less numerical approach is utilized to solve Euler's equation that is the governing equation of the irrotational flow of ideal fluids. A fractional step method of discritization is applied which consists to split each time step in two steps. This numerical method is based on moving-particle semi-implicit method (MPS) for simulating incompressible inviscid flows with free surfaces. The motion of each particle is calculated through interactions with neighboring particles covered with the kernel function. There are limitations for getting a stable solution by MPS method. In this paper, various kernel functions are considered and applied to improve the stability of MPS method. Based on these studies a kernel function is introduced that improves the stability of MPS method. The numerical results of the model are in good agreement with experimental results. The applicability of this model to simulate hydraulic problems with free surface is shown through the solution of dam break problem. The present method is a very useful utility for solving problems with irregular free surface in hydraulic and coastal engineering when an accurate prediction of free water surface is required.

Keywords: Numerical method; Free surface flow; Moving-particle semi-implicit method; Lagrangian approach

1. Introduction

Free surface hydrodynamic flows are of significant industrial and environmental importance but are difficult to simulate because the surface boundary conditions are specified on an arbitrarily moving surface.

* Corresponding author. Fax: +98 21 601 4828.
E-mail address: ataie@sharif.edu (B. Ataie-Ashtiani).

0169-5983/$30.00
doi:10.1016/j.fluiddyn.2005.12.002

In spite of the recent advances in numerical modeling of free surface flows, still there are difficulties to analyze problems in which the shape of the interface changes continuously or fluid–structure interactions where large deformations should be considered.

Recently, particle methods have been used in which each particle is followed in a Lagrangian manner. Moving interfaces and boundaries can be analyzed by mesh-less methods much easier than with the conventional finite element methods because it is difficult to fit and move a grid continuously. Furthermore, in Lagrangian formulations the convection terms are calculated by the motion without any numerical diffusion. The first ideas in this way were proposed by Monaghan (1988, 1994) for the treatment of astrophysical hydrodynamic problems with the method called smooth particle hydrodynamics (SPH) in which kernel approximations are used to interpolate the unknowns. This method was later generalized to fluid mechanic problems. Shao and Lo (2003) used the method of incompressible SPH for simulating Newtonian flows with free surface. This method was tested by typical two-dimensional (2D) dam break problem. The computations were in good agreement with available experimental data. The impact of a single wave generated by a dam break with a tall structure was modeled with a 3D version of the smoothed particle hydrodynamics method by Go'mez-Gesteira and Dalrymple (2004).

A modified particle method, called the moving-particle semi-implicit (MPS) method was proposed by Koshizuka and Oka (1996) and Koshizuka et al. (1998). In the MPS method, fluid is represented by moving particles. Convection is calculated by the motion of these particles. Thus, numerical diffusion, which is a problem in finite difference method, does not take place. The interfaces are always clear even if fragmentation or merging of the fluid occurs. This method has shown better stability in comparison with SPH method.

Independently a family of methods called meshless finite element methods (MFEM) has been developed. These methods use the idea of polynomial interpolants which fits a number of points minimizing the distance between the interpolated function and the value of the unknown point. MFEM was quite successfully applied for simulating free-surface fluid problems (Idelsohn et al., 2001). This method provides a proper performance and stability in comparison with other available meshless methods.

In spite of the successful applications of MPS method, still there are limitations for getting a stable solution by this method. In this paper, the application of MPS method for free surface problems in hydrodynamics and hydraulics is re-visited. A numerical model based on MPS method is developed and the performance of six different kernel functions is compared. Collapse of water column experiment is used for the numerical results verification and comparison. Based on these studies a new kernel function is introduced which improves the stability of MPS method.

2. Mathematical and numerical formulations

The governing equations of non-viscous flow which includes the mass conservation and momentum conservation are presented in Eqs. (1) and (2).

$$\frac{1}{\rho}\frac{D\rho}{Dt} = -\nabla.\mathbf{u}, \tag{1}$$

$$\frac{Du}{Dt} = -\frac{1}{\rho}\nabla p + \mathbf{f}, \tag{2}$$

Table 1
Different kernel functions

Kernel function	Kernel function formulation	Reference
KF1	$w(r)=\begin{cases} e^{-(r/\alpha r_e)^2} & 0\leqslant r\leqslant r_e \\ 0 & r_e<r \end{cases}$	Belytschko et al. (1996)
KF2	$w(r)=\begin{cases} \frac{2}{3}-4\left(\frac{r}{r_e}\right)^2+4\left(\frac{r}{r_e}\right)^3 & 0\leqslant r\leqslant \frac{r_e}{2} \\ \frac{4}{3}-4\left(\frac{r}{r_e}\right)+4\left(\frac{r}{r_e}\right)^2-\frac{4}{3}\left(\frac{r}{r_e}\right)^3 & \frac{r_e}{2}<r\leqslant r_e \\ 0 & r_e<r \end{cases}$	Belytschko et al. (1996)
KF3	$w(r)=\begin{cases} 1-6\left(\frac{r}{r_e}\right)^2+8\left(\frac{r}{r_e}\right)^3-3\left(\frac{r}{r_e}\right)^4 & 0\leqslant r\leqslant r_e \\ 0 & r_e<r \end{cases}$	Belytschko et al. (1996)
KF4	$w(r)=\begin{cases} -2\left(\frac{r}{r_e}\right)^2+2 & 0\leqslant \frac{r}{r_e}<\frac{1}{2} \\ \left(2\frac{r}{r_e}-2\right)^2 & \frac{1}{2}\leqslant \frac{r}{r_e}<1 \\ 0 & r_e\leqslant r \end{cases}$	Koshizuka and Oka (1996)
KF5	$w(r)=\begin{cases} \frac{r_e}{r}-1 & 0\leqslant r<r_e \\ 0 & r_e\leqslant r \end{cases}$	Koshizuka et al. (1998)
KF6	$w(r)=\begin{cases} \frac{40}{7\pi r_e^2}\left(1-6\left(\frac{r}{r_e}\right)^2+6\left(\frac{r}{r_e}\right)^3\right) & 0\leqslant r<0.5r_e \\ \frac{10}{7\pi r_e^2}\left(2-2\frac{r}{r_e}\right)^3 & 0.5r_e<r<r_e \\ 0 & r>r_e \end{cases}$	Shao and Lo (2003)

where $\rho(\mathrm{ML}^{-3})$ is the density, $\mathbf{u}(\mathrm{LT}^{-1})$ is the velocity vector, p $(\mathrm{ML}^{-1}\mathrm{T}^{-2})$ is the pressure and $\mathbf{f}(\mathrm{LT}^{-2})$ is the acceleration of body forces.

In particle methods, mass and momentum conservation equations are transformed to particle interaction equations. All interactions between particles are limited to a finite distance. The weight of interaction between two particles that are distance r apart can be described by a kernel function. In this paper six different types of kernel functions are considered. Three commonly used kernel (weight) functions are the Exponential (KF1), the Cubic Spline (KF2) and the Quartic Spline (KF3). Koshizuka and Oka (1996) proposed a kernel function (KF4) for simulating incompressible, viscid flows using MPS method. A modified kernel function (KF5) was later proposed by Koshizuka et al. (1998) for simulating incompressible, inviscid flows using MPS method. These kernel functions are also considered in this paper. Finally, the kernel function which was proposed by Shao and Lo (2003) for simulating Newtonian and non-Newtonian flows with a free surface using incompressible SPH method is considered. This kernel function is modified for use in MPS method (KF6). All of these kernel functions are given in Table 1.

In these functions, r is the distance between two particles i and j. Since the area that is covered with these kernel functions is bounded, a particle interacts with a finite number of neighboring particles. The radius of the interaction area is determined by parameter r_e and is called kernel size. A larger kernel size leads to more particles for interactions (Fig. 1).

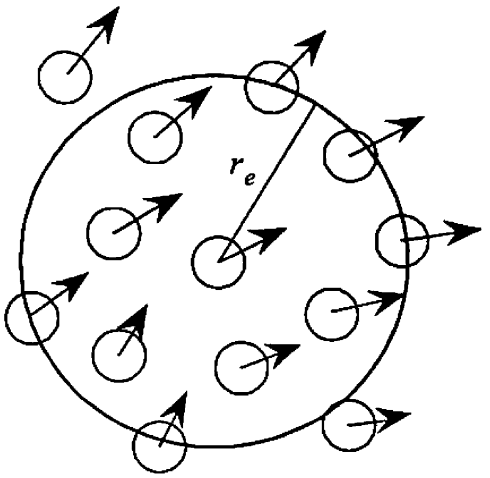

Fig. 1. Particle interaction within weight function.

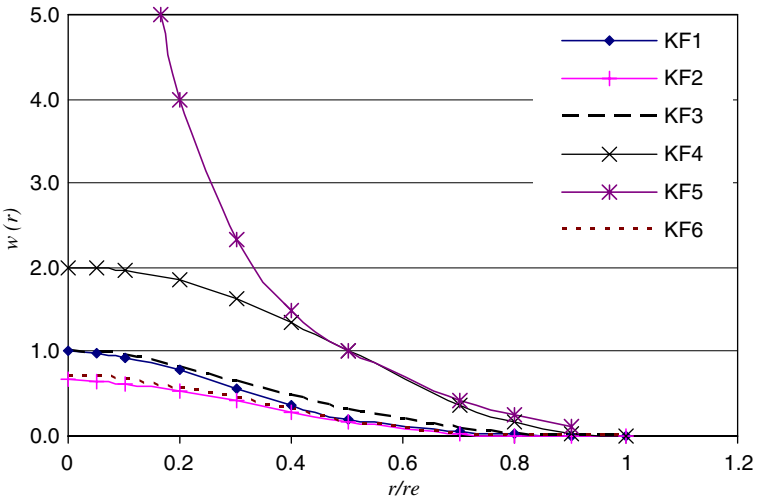

Fig. 2. Comparison between different kernel functions.

As illustrated in Fig. 2 all the kernel functions except KF5 that is infinity at $r = 0$, have a finite value at $r = 0$, the value of the functions gradually decrease and is zero at $r = r_e$. KF6 has a different characteristic; its value depends on the value of the radius of the interaction area. Fig. 2 shows the shape of these kernel function when $r_e = 2l_0$. Fig. 3 shows that the value of KF6 versus the value of r_e. As shown, the diagrams have same trajectories from $r = 0$ to $r = r_e$.

The particle number density can be computed as

$$\langle n \rangle_i = \sum_{i \neq j} w(|r_j - r_i|). \tag{3}$$

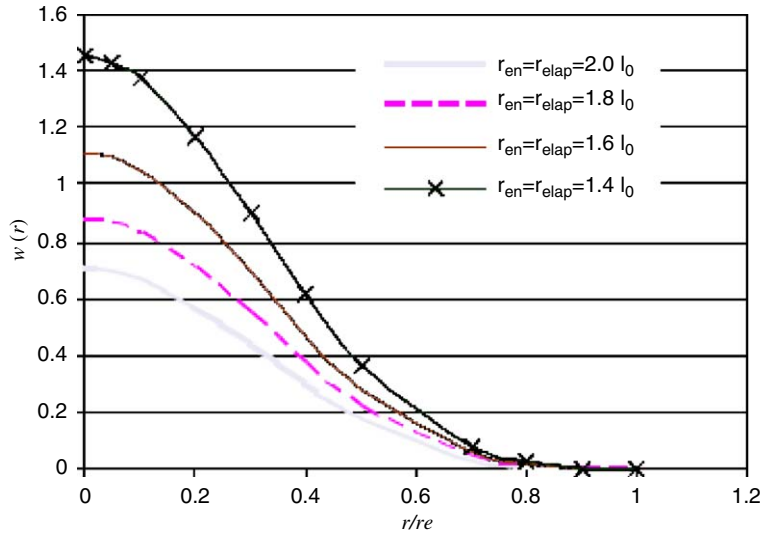

Fig. 3. Shape of KF6 for different r_e.

In this equation, the contribution from particle i itself is not considered. When the number of particles in a unit volume is denoted by N_i, the relation between n_i and N_i is written as

$$\langle N\rangle_i = \frac{\langle n\rangle_i}{\int_V w(r)\,\mathrm{d}v}. \tag{4}$$

The denominator of Eq. (4) is the integral of the kernel in the whole region, excluding a central part occupied by particle i. Assuming that the particles have the same mass m, we can see that the fluid density is proportional to the particle number density:

$$\langle \rho\rangle_i = m\langle N\rangle_i = \frac{m\langle n\rangle_i}{\int_V w(r)\,\mathrm{d}v}. \tag{5}$$

Thus, the continuity equation is satisfied if the particle number density is constant. This constant value is denoted by n^0 (Koshizuka and Oka, 1996). If ϕ and u are arbitrary scalar and vector, respectively, particle interaction models for differential operators are expressed as (Koshizuka et al., 1998)

$$\langle \nabla\phi\rangle_i = \frac{d}{n^0}\sum_{i\neq j}\frac{\phi_j-\phi_i}{|r_j-r_i|^2}(r_j-r_i)w(|r_j-r_i|), \tag{6}$$

$$\langle \nabla^2\phi\rangle_i = \frac{2d}{\lambda n^0}\sum_{i\neq j}[(\phi_j-\phi_i)w(|r_j-r_i|)], \tag{7}$$

where d is the number of space dimensions, n^0 is a particle number density fixed for incompressibility and λ is (Koshizuka et al., 1998):

$$\lambda = \frac{\int_V w(r) r^2 \, \mathrm{d}v}{\int_V w(r) \, \mathrm{d}v}. \tag{8}$$

The gradient model is obtained as the average of gradient vectors which are determined between particle i and its neighboring particles j.

The Laplacian model is derived from the physical concept of diffusion. Part of a quantity at particle i is distributed to neighboring particles j. Parameter λ is introduced to keep the same variance increase as that of the analytical solution. The current model of Laplacian is conservative since the quantity lost by particle i is obtained by particles j.

3. The time splitting

Since the time integration of Eqs. (1) and (2) presents some difficulties when the fluid is incompressible or near incompressible, a fractional step method has been proposed which consists to split each time step in 2 steps as follows (Zienkiewicz and Codina, 1995):

$$\frac{Du}{Dt} = \frac{u^{n+1} - u^n}{\Delta t} = \frac{u^{n+1} - u^* + u^* - u^n}{\Delta t} = \frac{\Delta u' + \Delta u^*}{\Delta t}, \tag{9}$$

$$\frac{D\rho}{Dt} = \frac{\rho^{n+1} - \rho^n}{\Delta t} = \frac{\rho^{n+1} - \rho^* + \rho^* - \rho^n}{\Delta t} = \frac{\Delta \rho' + \Delta \rho^*}{\Delta t}, \tag{10}$$

where $\Delta t = t^{n+1} - t^n$ is the time step; $u^n = u(t^n, x^n)$, $\rho^n = \rho(t^n, x^n)$ and ρ^* and u^* are fictitious variables defined by the split.

From Eqs. (1) and (9):

$$\frac{\Delta u'}{\Delta t} + \frac{\Delta u^*}{\Delta t} = -\frac{1}{\rho}\nabla p + f, \tag{11}$$

$$\frac{\Delta u^*}{\Delta t} = f,$$

$$\frac{\Delta u'}{\Delta t} = -\frac{1}{\rho}\nabla p. \tag{12}$$

From Eqs. (2) and (10)

$$\frac{1}{\rho}\left(\frac{\Delta \rho'}{\Delta t} + \frac{\Delta \rho^*}{\Delta t}\right) = -\nabla.[u^{n+1} - u^* + u^*], \tag{13}$$

$$\frac{1}{\rho}\frac{\Delta \rho^*}{\Delta t} = -\nabla.u^*,$$

$$\frac{1}{\rho}\frac{\Delta \rho'}{\Delta t} = -\nabla.\Delta u'. \tag{14}$$

Continuity equation requires that the fluid density should be constant. According to Eq. (5), this is equivalent to the particle number density being constant, n^0. When the particle number density n^* is not n^0, it is implicitly corrected to n^0 by

$$n^* + \Delta n' = n^0. \tag{15}$$

Thus according to Eq. (15) we have

$$\frac{1}{n^0}\frac{\Delta n'}{\Delta t} = -\nabla.\Delta u'. \tag{16}$$

The velocity correction value is also derived from the implicit pressure gradient term as

$$\Delta u' = -\frac{\mathrm{d}t}{\rho}\nabla p^{n+1}. \tag{17}$$

With Eqs. (15)–(17), a Poisson equation of pressure is obtained:

$$\langle \nabla^2 p^{n+1}\rangle_i = -\frac{\rho}{\mathrm{d}t}\frac{\langle n^*\rangle_i - n^0}{n^0}. \tag{18}$$

The right-hand side is represented by the deviation of the particle number density from the constant value, while it is usually velocity divergence in grid methods. The left-hand side of Eq. (18) is discretized by the Laplacian model as given by Eq. (7). Finally, we have simultaneous equations expressed by a linear symmetric matrix.

The MPS can be summarized in a simple algorithm, combined of 6 steps.

1. Initialize fluid: $\mathbf{u}^0$, $\mathbf{r}^0$.
   For each time step $\mathrm{d}t$:
2. Compute forces and apply them to particles. Find temporary particle positions and velocities $\mathbf{u}^*$, $\mathbf{r}^*$

$$\mathbf{u}^* = \mathbf{u}^n + \Delta t\mathbf{f}, \tag{19}$$

$$\mathbf{r}^* = \mathbf{r}^n + \mathbf{u}^*\Delta t. \tag{20}$$

3. Compute particle number density n^* using new particle locations.
4. Solve Poisson equation of pressure after discretizing it into a system of linear equations.
5. Compute velocity correction $\Delta u'$ from the pressure equation

$$\Delta u' = -\frac{\mathrm{d}t}{\rho}\nabla p^{n+1}. \tag{21}$$

6. Compute new particle positions and velocities

$$u^{n+1} = u^* + \Delta u', \tag{22}$$

$$r^{n+1} = r^n + u^{n+1}\Delta t. \tag{23}$$

End for.

The particle density number decreases for particles on the free surface. A particle which satisfies a simple condition $n_i^* < \beta n^0$ is considered on the free surface (Young Yoon et al., 2002). Pressure $p = 0$

(or atmospheric pressure, if applicable) is applied to these particles on the free surface in the pressure calculation. Solid boundaries such as walls or other fixed objects are represented by fixed particles. Velocities are always zero at these particles. Three layers of particles are used to represent fixed objects to ensure that particle density number is computed accurately and the particles on the inner first line of walls are involved in the pressure calculations.

4. Model application

4.1. Broken dam analysis

Dam-break flows are an important practical problem in civil engineering and their prediction is now a required element in the design of a dam and its surrounding environment. The idealized 2D problem of the instantaneous removal of a barrier between two bodies of water at rest which is a model of dam break, has been used as a verification problem of the codes for the free surface (Stansby et al., 1998). In order to show the ability of MPS method to simulate fragmentation and coalescence of the fluid, a vertical wall has also been located on the right-hand side. The geometry is described in Fig. 4. The test calculations of this problem are also used to investigate parameters used in particle interaction models of MPS method. Thus, sensitivity analyses have been performed in order to obtain the most effective value for each calculation parameter, so that the calculated shape of the free surface agrees well with the experimental results and there is balance between computation time and accuracy (Farhadi, 2003).

The calculation parameters are the following:

Initial distance between neighboring points, $l_0 = 0.8\,\text{cm}$.

Free surface parameter, $\beta = 0.97$.

Radius of kernel functions:

KF1: $r_e = 2.0 l_0$,

KF2: $r_e = 2.0 l_0$,

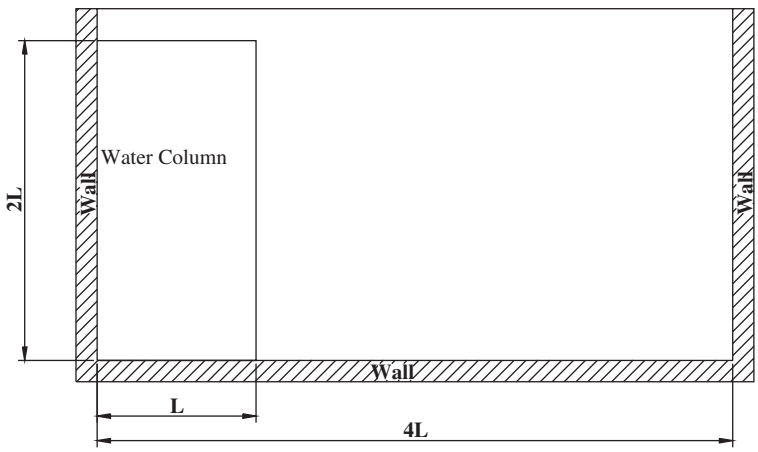

Fig. 4. Geometry of the collapse of water column.

KF3: $r_e = 1.8l_0$,
KF4: $r_e = 1.5l_0$,
KF5: $r_{en} = 2.1l_0$, : $r_{elap} = 4.0l_0$,
KF6: $r_e = 2.0l_0$.

Courant number $Cr = \dfrac{\Delta t|u|}{l_0} \leqslant 0.2$,

Maximum $\Delta t \leqslant 10^{-3}$,

where r_e is the radius of interaction (Kernel size). It is not necessary to use a common kernel size for all the three particle interaction models (Shao and Lo, 2003) which are particle number density, the pressure gradient term, and Laplacian of pressure. r_{en} is used in the particle number density and the pressure gradient term and r_{elap} is used in the Laplacian of pressure.

Fig. 5 shows a sensitivity analysis performed on kernel size in order to obtain the most effective value for this parameter when KF2 is used as the model's kernel function. A numerical explosion occurs when $r_{en} = r_{elap} \leqslant 1.3l_0$. If r_e is too small, the number of neighboring particles for interactions is too small for accurate and stable calculations. It is reasonable that there is a minimum limit of r_e for numerical stability. When $r_{en} = r_{elap} = 1.4l_0$ the water collapse simulation is stable before water impinges the right vertical wall. So by using this kernel size for the kernel function KF2 in MPS method, this method will not be able to simulate fragmentation and coalescence of the fluid. When $r_{en} = 1.5l_0$, $r_{elap} = 4.0l_0$, the number of particles on the free surface is abnormally high between 0.17 and 0.25 s. This means that numerical instability occurs but is suppressed.

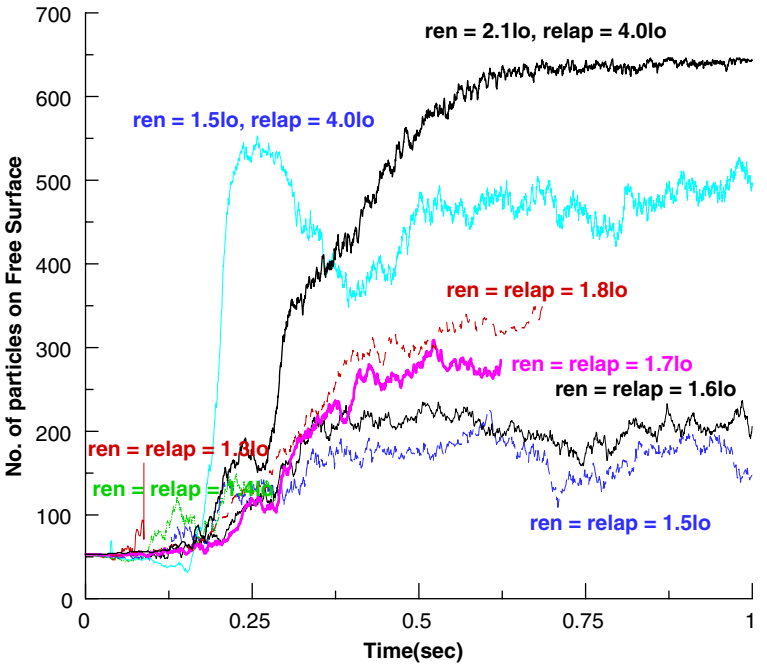

Fig. 5. Effect of kernel size used in KF2 kernel function.

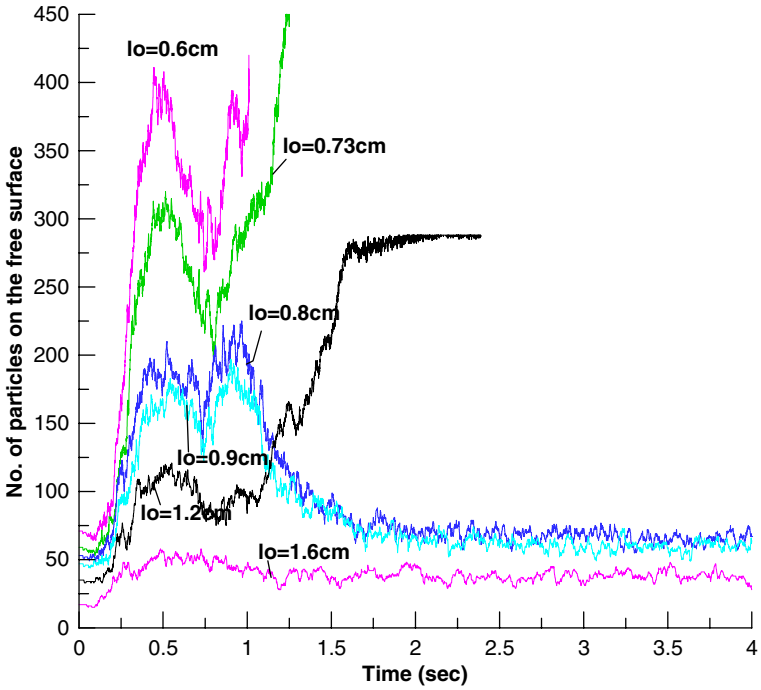

Fig. 6. Effect of particle size used in KF6 kernel function.

When $r_{en} = 2.1l_0$, $r_{elap} = 4.0l_0$, the particles are dispersed and a large number of particles are regarded to be on free surface such that after 0.5 s, nearly all the fluid particles are satisfying the free surface condition which is not an accurate simulation. The stability and accuracy of calculations are successful when $1.4 < r_{en} = r_{elap} \leqslant 1.8l_0$. Fragmentation and coalescence of fluid is simulated and the computations are stable during the simulation. The simulation is more stable when $r_{en}=r_{elap}=1.6l_0$ and $r_{en}=r_{elap}=1.5l_0$ such that the water column collapse can be simulated till water impinges the left vertical wall at 1 s. Our investigation also showed that by using $r_{en} = r_{elap} = 1.5l_0$, the simulation time is less than when $r_{en} = r_{elap} = 1.6l_0$ is used as the kernel size (Farhadi, 2003). That clears the reason $r_{en} = r_{elap} = 1.5l_0$ is selected as the kernel size for kernel function KF2 in MPS method.

Fig. 6 shows a sensitivity analysis performed on distance between neighboring points (or particle size), l_0, using KF6 kernel function. The results of simulating the collapse of water column at different times can be observed in Fig. 7. It is obvious that increasing the particle size will decrease the number of fluid particles involved in the simulation. As illustrated in Figs. 6 and 7, analysis show that a very low number of fluid particles will result in an inaccurate simulation while a large number of fluid particles will increase the simulation time. Thus a reasonable value for particle size should be selected. In this study $l_0 = 0.8$ cm which makes the simulation more stable, and results in a number of fluid particles which are a good representative of volume of fluid, is selected.

Similar approach has been used in order to find the most effective value for other calculation parameters.

The water column collapse is simulated with MPS method using different kernel functions introduced in Table 1. In all the simulations, the collapse starts at time $t = 0$, when the removable board is slid up.

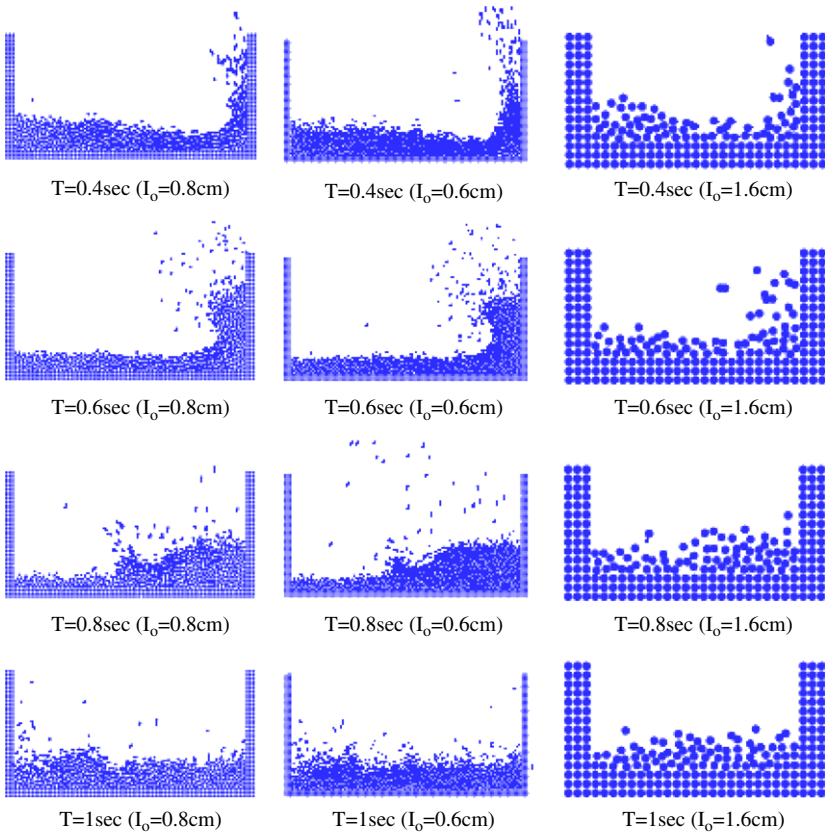

Fig. 7. Water column collapse using various particle sizes.

Table 2
Comparison between different kernel functions

Type of kernel	No. of time steps to simulate till 0.3 s	Time needed to simulate till 0.8 s	Average CPU time per time step	Successful simulation time(s)
KF1	414	1114	4.1	0.8
KF2	422	1099	4.41	1
KF3	413	1147	4.28	1
KF4	392	1026	4.25	0.8
KF5	437	2221	4.14	—
KF6	426	1098	4.52	>4

The water runs in the bottom wall until, near 0.3 s, it impinges on the right vertical wall and changes its direction. At time $t = 1$ s the water reaches the left vertical wall again.

The summarized results of comparison between different kernel functions are given in Table 2. According to the results and as illustrated in Table 2, by using the kernel function KF4, instability does not

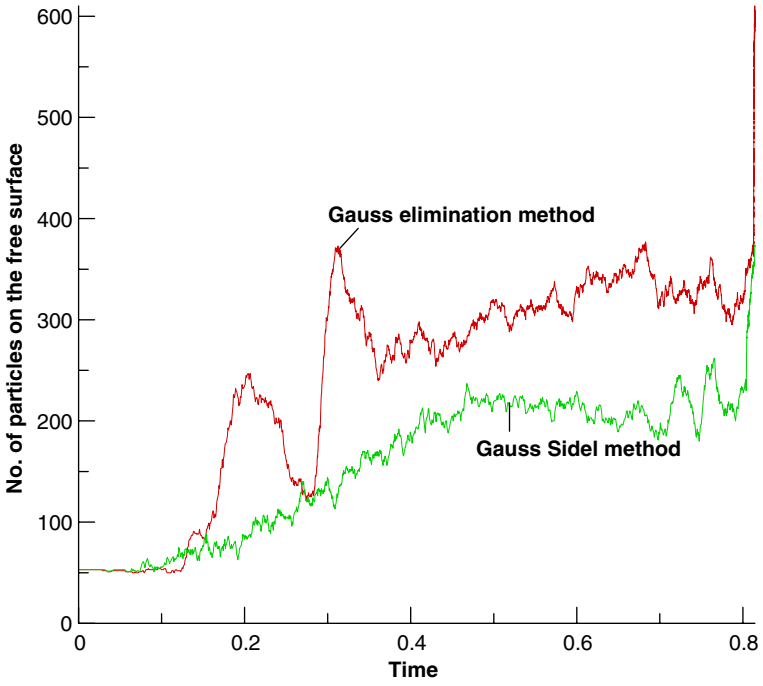

Fig. 8. Effect linear equation solvers on number of particles on the free surface for KF5 kernel function.

occur until 1 s. But the shape of the free surface is not consistent with the experimental results after 0.8 s. This kernel function needs the less computation time amongst other kernel functions.

KF2 and KF3 successfully simulated the collapse of water column until 1s, but after water impinges the left vertical wall instability occurs. The results of numerical calculation are not in good agreement with the experimental results (Koshizuka and Oka, 1996) after 0.8 s if KF1 is used.

In our investigation we have concluded that by using KF5 kernel function, the method used for solving the system of linear equations of $AX = b$ significantly influences the numerical stability and computation time of the MPS method, especially for modeling the fragmentation and coalescence of water after it impinges the right vertical wall. Two different methods of Gauss elimination and Gauss–Seidel linear equation solver are considered in this work. According to our studies if we use Gauss elimination method for solving the linear equation of $AX = b$, the particles are dispersed and a large number of particles are regarded as the free surface. By using Gauss–Seidel method and inserting an artificial error in to the solution, this problem is solved, as shown in Fig. 8.

KF6 successfully simulated the collapse of water column for more than 4 s, when the water becomes horizontal inside the container. Agreement with the experimental results of Koshizuka and Oka (1996) who carried out an experimental in the same geometry (Fig. 4), showing the collapse of water column till 1 s are excellent (Fig. 9). At 0.4 s, the water goes up losing its momentum, at 0.5 s it begins to come down. A breaking wave is observed at 0.7 s and the wave falls down in to the remaining water at 0.8 s. A new reflected wave flies toward the left at 0.9 s reaching the left wall near the first second of the process. The motion of the leading edge using different radius for Kernel Function KF6 is compared with the experimental results of Koshizuka and Oka (1996) in Fig. 11. The good agreement between

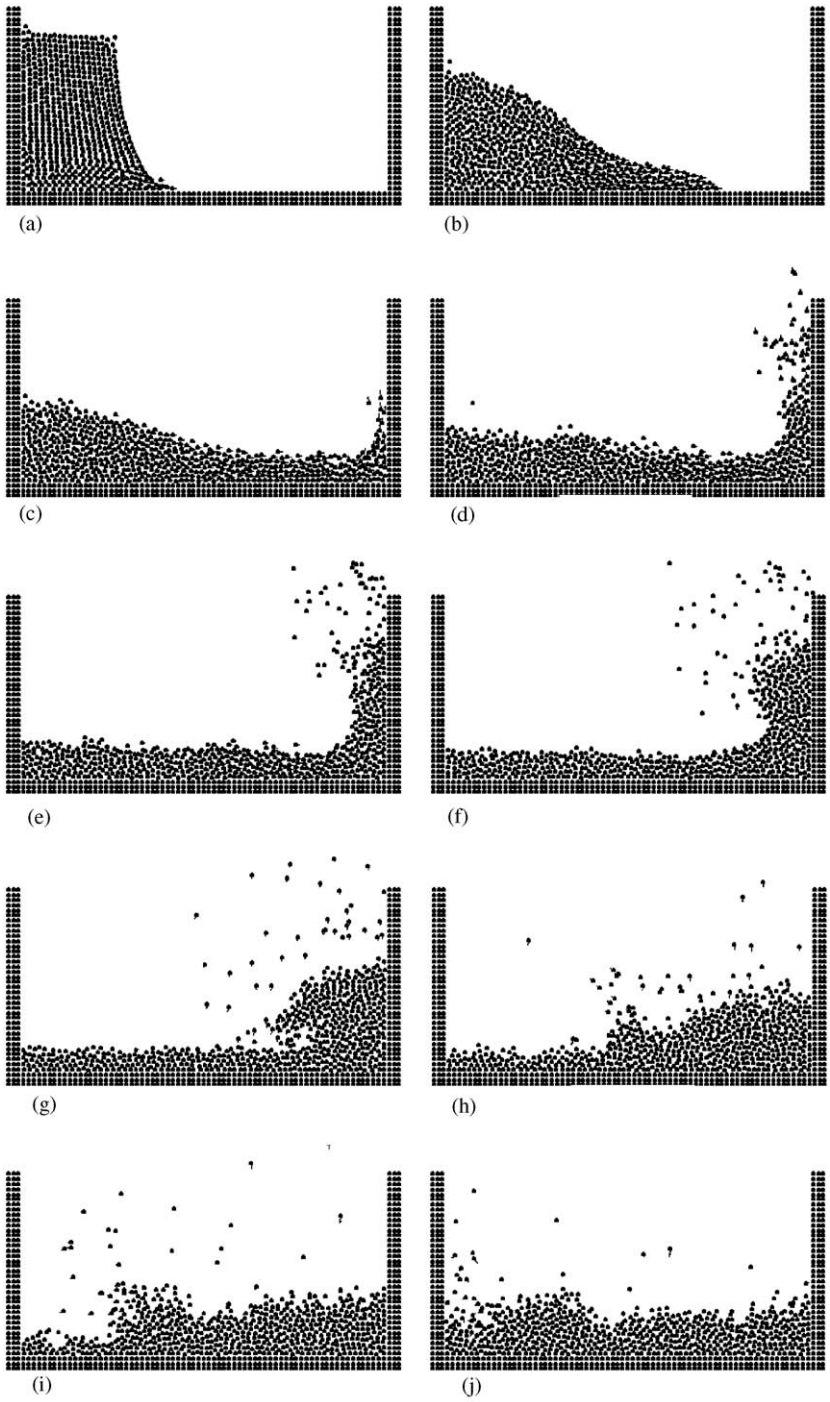

Fig. 9. Numerical simulation of water column collapse: (a) $t = 0.1$ s, (b) $t = 0.2$ s, (c) $t = 0.3$ s, (d) $t = 0.4$ s, (e) $t = 0.5$ s, (f) $t = 0.6$ s, (g) $t = 0.7$ s, (h) $t = 0.8$ s, (i) $t = 0.9$ s and (j) $t = 1$ s.

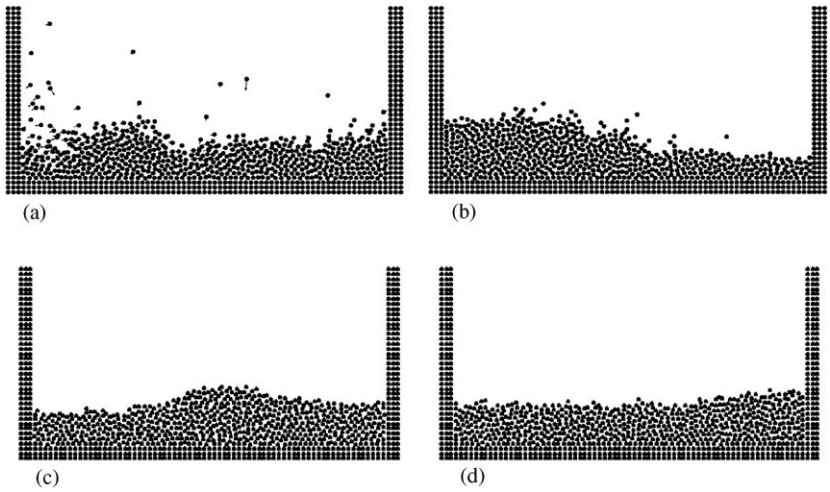

Fig. 10. Water column collapse simulation after: (a) $t = 1$ s, (b) $t = 1.37$ s, (c) $t = 2.15$ s and (d) $t = 3.13$ s.

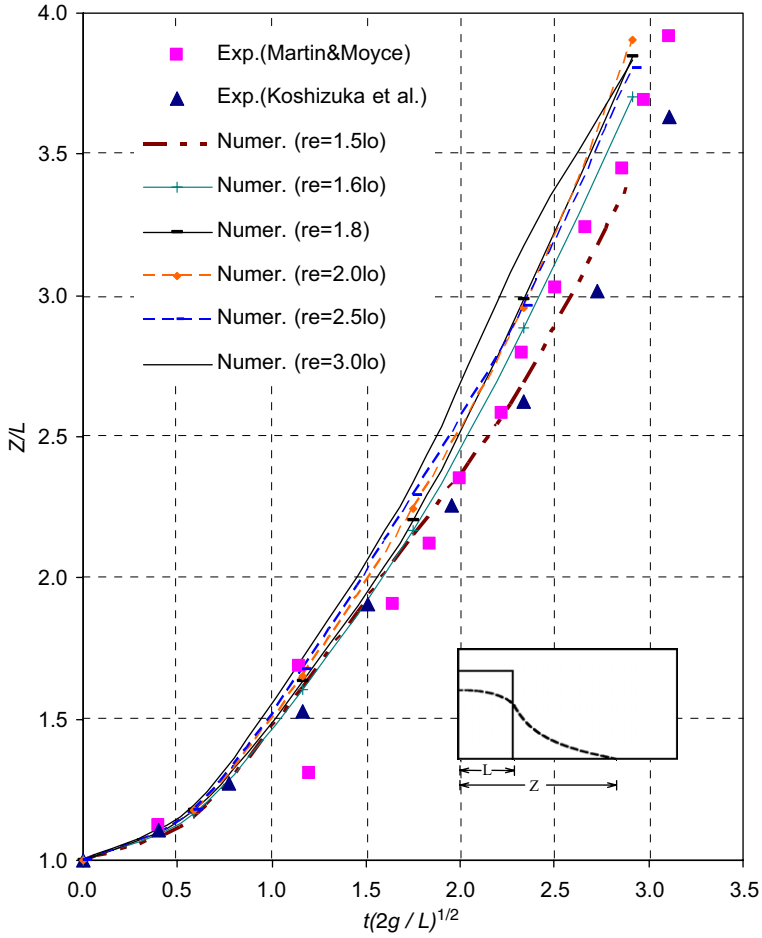

Fig. 11. Comparing the motion of leading edge with experimental results (■ Exp. (Martin and Moyce, 1952); ▲ Exp. (Koshizuka et al., 1998)).

numerical and experimental results is observed in this figure. After water impinges the left wall (after 1 s) the collapse of water column is still successfully simulated until water loses all its momentum and becomes completely horizontal inside the container (Fig. 10, Table 2). This is a remarkable ability and shows the stability improvement of MPS method using KF6 kernel function (Fig. 11). In previous studies Koshizuka and Oka (1996) improved MPS method and were successful to simulate water column collapse until water impinges the left vertical wall at about 1 s, but after that instability occurred. The success of KF6 kernel function is supported by a large number of numerical simulations that have been performed for sensitivity analyses (Farhadi, 2003).

5. Conclusions

The paper presents application of MPS method to simulate incompressible inviscid flows with free surfaces. The method employs particles to discretize the Euler equations and the interactions among particles simulate the flows. Six different kernel functions are presented. Collapse of water column is considered and in order to show the good ability of MPS method to simulate fragmentation and coalescence of the fluid, a vertical wall has been located on the right side. The kernel function proposed by Shao and Lo (2003) for simulating free surface water using SPH is found to considerably improve the stability of MPS method. By using this kernel function, the collapse of water column was successfully simulated until the water looses all its momentum and becomes completely horizontal inside the container. This is a remarkable ability amongst other particle methods.

Nomenclature

Cr	Courant number
d	number of space dimensions
$\mathbf{f}$	acceleration of body forces (LT^{-2})
l_0	initial distance between neighboring points (particle size) (L)
n^0	initial particle number density
n	particle number density
$\Delta n'$	particle number density correction
n^*	fictitious particle number density
N_i	number of particles in a unit volume
p	pressure ($ML^{-1}T^{-2}$)
r	distance between two particles (L)
r_e	radius of the interaction area (L)
$\mathbf{u}$	velocity vector (LT^{-1})
v	velocity vector (LT^{-1})
w	velocity vector (LT^{-1})
u^*	fictitious velocity
$\Delta u'$	velocity correction (LT^{-1})
β	free surface parameter

λ non-dimensional parameter, used to keep the same variance increase as that of analytical solutions
ρ density (ML^{-3})
ρ^* fictitious density (ML^{-3})
V volume (L^3)

References

Belytschko, T., Krongauz, Y., Organ, D., Fleming, M., Krysl, P., 1996. Meshless methods: an overview and recent developments. Comput. Methods Appl. Mech. Eng. 139, 3–47.

Farhadi, L., 2003. Numerical modeling of irregular free surface flow using a fully Lagrangian method. M.Sc. Thesis, Department of Civil Engineering, Sharif University of Technology, 154p.

Go'mez-Gesteira, M., Dalrymple, R.A., 2004. Using a three-dimensional smoothed particle hydrodynamics method for wave impact on a tall structure. J. Waterway Port Coastal Ocean Eng. 130 (2), 63–69.

Idelsohn, S.R., Storti, M.A., Onate, E., 2001. Lagrangian formulation to solve free surface incompressible inviscid fluid flows. Comput. Methods Appl. Mech. Eng. 191, 583–593.

Koshizuka, S., Oka, Y., 1996. Moving-particle semi-implicit method for fragmentation of incompressible fluids. Nucl. Sci. Eng. 123, 421–434.

Koshizuka, S., Nobe, A., Oka, Y., 1998. Numerical analysis of breaking waves using the moving particle semi-implicit method. Int. J. Numer. Methods Fluids 26, 751–769.

Martin, J.C., Moyce, W.J., 1952. An experimental study of the collapse of liquid columns on a rigid horizontal plane. Philos. Trans. R. Soc. London Ser. A, 244–312.

Monaghan, J.J., 1988. An introduction to SPH. Comput. Phys. Commun. 48, 89–102.

Monaghan, J.J., 1994. Simulating free surface flows with SPH. J. Comput. Phys. 110, 399–406.

Shao, S., Lo, E.Y.M., 2003. Incompressible SPH method for simulating Newtonian and non-Newtonian flows with a free surface. Adv. Water Resour. 26, 787–800.

Stansby, P.K., Chegini, A., Barnes, T.C.D., 1998. Initial stages of dam-break flow. J. Fluid Mech. 370, 203–220.

Young Yoon, H., Koshizuka, S., Oka, Y., 2002. A particle-gridless hybrid method for incompressible flows. Int. J. Numer. Methods Fluids 30, 407–424.

Zienkiewicz, O.C., Codina, R., 1995. A general algorithm for compressible and incompressible flow, Part I: the split, characteristic-based scheme. Int. J. Numer. Methods Fluids 20, 869–885.